ISSN:2790-1688 DOI: 10.56028/aetr.2.1.31

Experimental study on seismic performance of steel-concrete connection section of receiver tower of CSP station

Tengfei Chu[1], Guoliang Bai[1,*] and Jiarui Li[1]

1School of Civil Engineering, Xi' an University of Architecture and Technology, Xi' an 710055, China

*Corresponding author e-mail: guoliangbai@126.com

Abstract. Taking the actual structure of the solarreceiver tower of a 243m high optical thermal power station as the prototype, and fully considering the influence range of structural quality and stiffness mutation, the 180-221m steel-concrete connection section structure is selected as the research object. The equivalent scale model is designed and manufactured according to the scale ratio of 1:8, and the quasi-static test under low cyclic reciprocating load is carried out. The failure characteristics, hysteretic performance, skeleton curve, stiffness and strength degradation, energy dissipation capacity, ductility and bearing capacity of the connection section structure are studied. The results show that the ultimate failure of the connection section structure is the overall bending yield of the upper steel frame and the local failure of the steel-concrete connection joint; The stiffness and strength of the connection section degenerate seriously when the structure is damaged. The equivalent viscous damping coefficient is 0.261 and the displacement ductility coefficient is 9.2, indicating that the specimen has good energy dissipation capacity and ductility under earthquake; The special joint structure can ensure the reliable connection between the upper steel frame and the lower concrete and meet the safety requirements.

Keywords: receiver tower; vertical mixed structure; steel-concrete connection section; pseudo-static test; seismic performance

1. Introduction

As an inexhaustible and inexhaustible clean energy, solar energy can be used for solar power generation to effectively solve the shortage of electric energy resources and the environmental pollution caused by thermal power generation [1,3]. At present, there are few research literatures on the seismic performance test of steel-concrete hybrid receiver tower structures at home and abroad, and the general research objects are mostly similar towering structures. Guo Feng et al. [4] studied the seismic performance of the overall structure of the hybrid receiver tower, but did not involve the detailed analysis and design of the connection section. This research group [5,10] conducted a 1/18 scale shaking table test on a large-scale steel-concrete vertical hybrid receiver tower structure with a height of 243m, and studied the seismic performance of the overall structure of the steel-concrete receiver tower. The mixed connection section is subjected to complex forces, and the mass and stiffness are suddenly changed, which is the weak link of the receiver tower, which should be further studied and analyzed.

In order to study the seismic performance of the connecting section structure of large-scale steel-concrete vertical hybrid receiver tower in CSP station, the low-cycle reciprocating loading was carried out on the steel-concrete connecting-section structure of receiver tower in CSP station with a scale ratio of 1/8. In the test, the failure characteristics, hysteretic performance, skeleton curve, stiffness degradation, strength degradation and other seismic performance indicators of the connection structure were analyzed.

2. Test program

2.1 Specimen design

The total height of the main structure of the steel-concrete receiver tower is 243m, and according to the previous shaking table test results of our research group, taking full account of the influence

ISSN:2790-1688 DOI: 10.56028/aetr.2.1.31
range of mass and stiffness mutation, the connection segment structure with a structural height of 180-221m is selected as the research object.

Considering the weight and height restrictions of laboratory test site and test hoisting, the test scale ratio is determined to be 1:8. The steel structure is simplified according to the equivalent lateral stiffness, and the reinforcement of the cylinder is designed according to the bending of the normal section and the shear of the inclined section. The structural design of the connection section is shown in Figure 1.

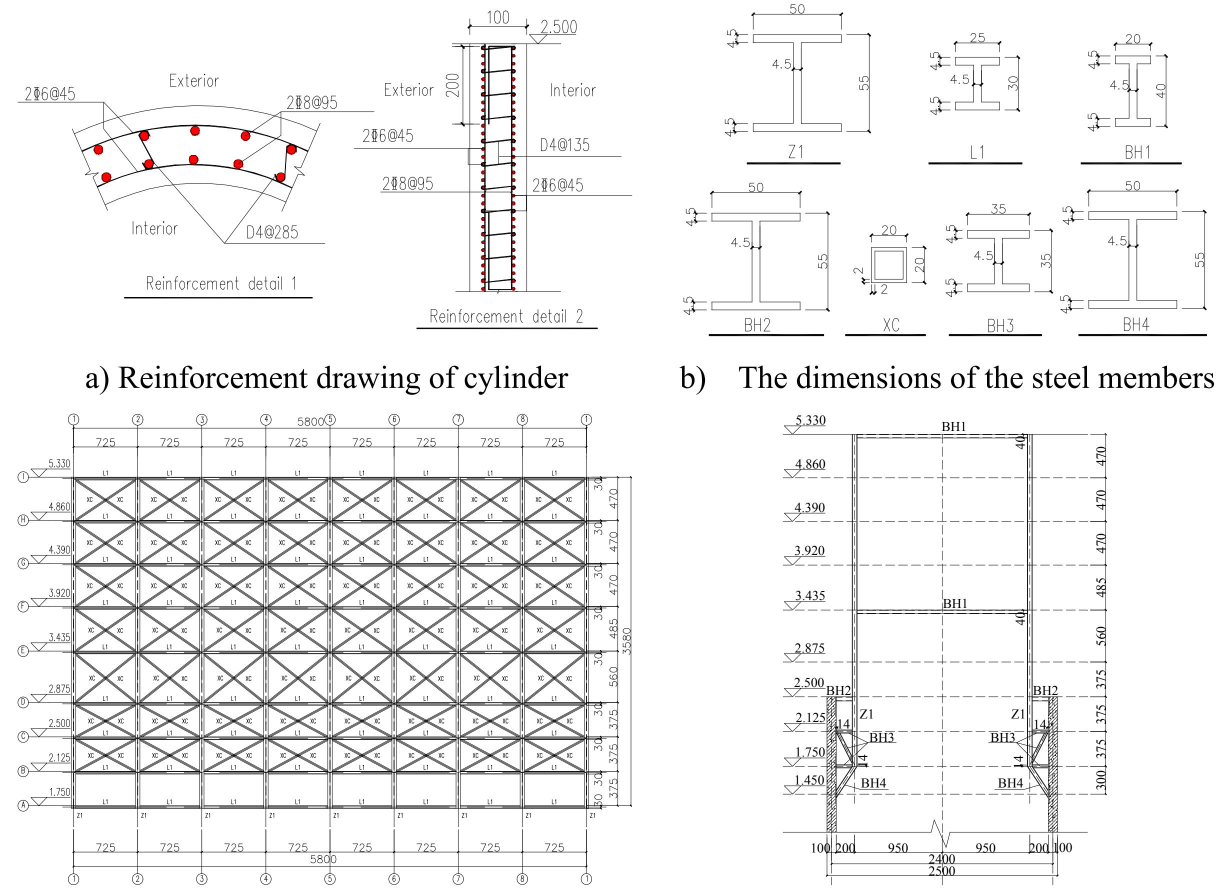

a) Reinforcement drawing of cylinder b) The dimensions of the steel members

c) Expanded drawing of steel structure d) Structure diagram of connecting section

Figure 1. Structural design of the connection section.

2.2 Material properties

According to the design of similarity relationship, C45 commercial concrete is adopted for concrete, HRB500 reinforcement is selected for reinforcement, and Q355 steel is used for steel frame. The test results of mechanical properties of concrete, reinforcement and steel materials are shown in Table 1 and Table 2.

Table 1. Mechanical properties of concrete.

Type	f_{cu}/MPa	f_c/MPa	f_t/MPa	E_c/MPa
C45	52.7	3.39	50.0	3.35×10^4

Table 2. Mechanical properties of steel.

Type	f_y/MPa	f_u/MPa	E_s/MPa
Q355	400.1	508.8	2.06×10^5
D8	534.2	704.1	2.0×10^5
D6	520.5	695.8	2.0×10^5

ISSN:2790-1688 DOI: 10.56028/aetr.2.1.31

2.3 Loading system

The MTS electro-hydraulic servo actuator system of the structure and earthquake resistance Laboratory of Xi'an University of architecture and technology is used for quasi-static test loading. The maximum force applied by the horizontal actuator is 1000KN, and the displacement range is ± 375mm. The test loading device is shown in Figure 2.

After calculation, the vertical load to be applied by the model is 112.5 kN. Keep the vertical load unchanged in the test, and then apply the horizontal cyclic load. Before the yield of the model, the loading shall be controlled according to the load mode. The initial loading shall be graded with 10kN as the level difference, and each level of load shall be cycled once. The initial cracking of the model shall be observed to determine the cracking load of the model; After the model yields (i.e. there is an obvious turning point in the model load displacement curve), the displacement control mode is changed. The yield displacement is the first level displacement, and then the displacement loading level difference is loaded by 2mm, 2mm, 10mm, 10mm, 20mm, 40mm and 40mm according to the site conditions. Each level of displacement is cycled for 3 times until the horizontal bearing capacity of the model drops to 85% of the peak load or the specimen has obvious signs of failure, the model is judged to be damaged and the loading is stopped.

Figure 2. Loading device of test model.

3. Experimental observations

When the horizontal load is loaded to 18t, the displacement is 12.05mm. It is observed that the slope of the load displacement hysteretic curve decreases slightly, and the strain of some steel members and reinforcement is close to the yield strain. It can be judged that the model structure begins to enter the elastic-plastic deformation stage. After that, the loading system adopts the displacement loading control mode.

During the cyclic loading with a displacement of ± 36.05mm and ± 56.05mm, the upper layer of No. 2 and No. 3 columns locally bulged, the connections of the third and fourth diagonal braces on both sides of No. 3 steel column were disconnected and out of plane instability occurred, and the third diagonal brace was broken during repeated loading, as shown in Figure 3 a). During the cyclic loading process with displacements of ±96.05mm and ±136.05mm, the cracks in the inner wall of the concrete cylinder further developed, most of the diagonal braces and horizontal beams of the upper steel frame were seriously damaged, and the steel columns were partially bulged and slightly twisted as shown in Figure 3 b). At this time, the horizontal load has dropped to below 85% of the peak load, and it is considered that the structural damage is serious and the loading is stopped. The failure results of the specimens are shown in Figure 3 c) below.

ISSN:2790-1688 DOI: 10.56028/aetr.2.1.31

a) Diagonal brace buckling	b) Torsion of steel column	c) Final failure mode

Figure 3. Experimental phenomenon of specimen.

4. Analysis of test results

4.1 Hysteretic curve

The load displacement hysteretic curve of the specimen is shown in Figure 4.

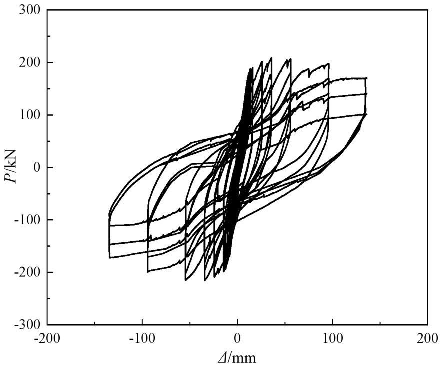

Figure 4. Hysteresis curve of specimen.

Where p is the horizontal load on the top of the specimen and Δ is the horizontal displacement on the top of the specimen..It can be seen from Figure 3 that the hysteretic curve of the model structure is in an inverse S-shape as a whole and has a certain energy dissipation capacity.

4.2 Skeleton curve

Connect the peak value points of each stage hysteretic loop of the model structure to obtain the skeleton curve of the structure, as shown in Figure 5.

It can be seen from Figure 5 that the model structure has experienced elastic stage, elastic-plastic stage and failure stage. With the continuous increase of loading displacement, the bearing capacity of the specimen decreases, the stiffness and strength degrade, and finally the specimen is damaged.

ISSN:2790-1688 DOI: 10.56028/aetr.2.1.31

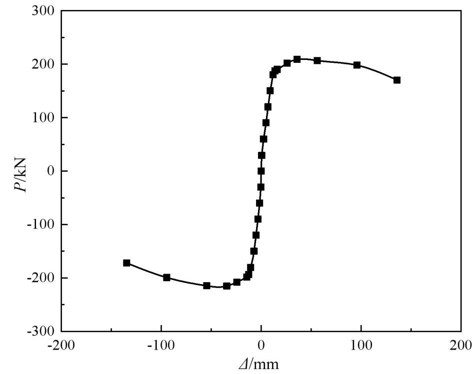

Figure 5. Skeleton curve of specimen.

4.3 Bearing capacity and ductility

According to the provisions of JGJ / T 101-2015[11], the characteristic value load of skeleton curve is calculated. In this paper, the ductility performance of the specimen is characterized by displacement ductility coefficient.

The calculation results of characteristic load and ductility coefficient are shown in Table 3. It can be seen from table 3 that the ductility coefficient of the model structure when it is damaged is 9.2, indicating that the structure still has a certain energy dissipation capacity after reaching the maximum bearing capacity, will not be suddenly damaged and has good deformation performance.

Table 3. Characteristic value and displacement ductility coefficient of specimen.

Yield point		Peak point		Ultimate point		Ductility coefficient
P_y	Δ_y	P_m	Δ_m	P_u	Δ_u	
kN	mm	kN	mm	kN	mm	
189.7	13.3	212.2	35.2	180.4	121.9	9.2

4.4 Strength and stiffness degradation

The strength degradation of the specimen is measured by the reduction degree λi of the bearing capacity in different cycles under the same level of loading and displacement. The stiffness of the specimen is represented by the secant stiffness K, which is the ratio of the first cycle peak load to the peak displacement of each stage of loading.

The relationship between the strength degradation rate and the loading displacement is shown in Figure 6 a), and the stiffness degradation curve is shown in Figure 6 b).

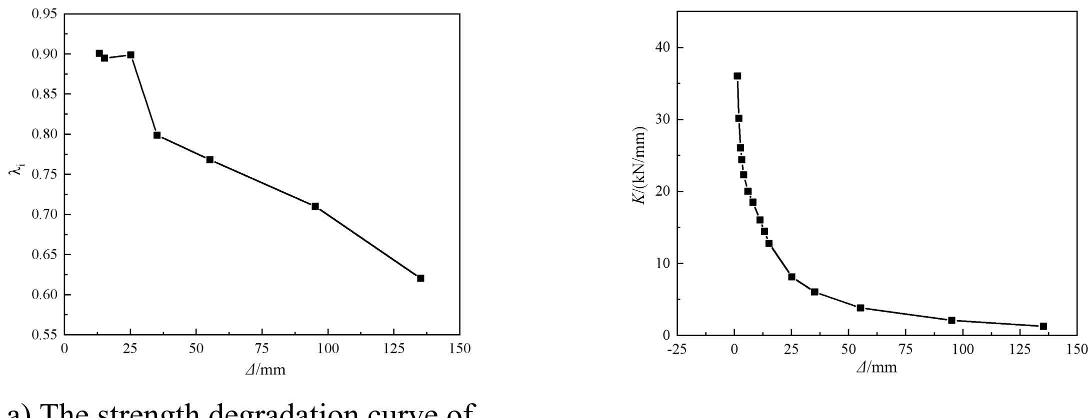

a) The strength degradation curve of specimen

b) Stiffness degradation curve of specimen

Figure 6. Degradation law of strength and stiffness of specimens.

ISSN:2790-1688 DOI: 10.56028/aetr.2.1.31

It can be seen from Figure 6 a) that the strength degradation rate reaches 0.62 when the specimen is damaged, and the strength degradation is severe. It can be seen from Figure 6 b) that with the increase of the loading displacement, the stiffness of the steel-concrete connection structure of the receiver tower of the CSP station decreases continuously. Rapidly, then the upper steel frame and the lower longitudinal reinforcement are partially buckled, and the decrease in stiffness begins to slow down. Finally, there are basically no new cracks in the structure, and the stiffness degradation tends to be stable.

4.5 Energy consumption capacity

The equivalent viscous damping coefficient he in JGJ 101-2015 is used to characterize the level of energy dissipation capacity. The greater the he value, the better the energy dissipation capacity of the structure [12]. The calculation results of energy consumption capacity are shown in Table 4.

Table 4. Calculation result of energy consumption capacity of specimen.

Eigenvalue point	Yield point	Peak point	Ultimate point
Equivalent viscous damping coefficient h_e	h_{ey}	h_{em}	h_{eu}
Calculated value	0.113	0.215	0.261

It can be seen from Table 4 that the equivalent viscous damping coefficient of the specimen gradually increases with the increase of loading displacement, and the growth rate gradually decreases, indicating that the damage of the structure gradually increases after yield, the plastic area gradually expands, absorbs a lot of energy, and the energy dissipation capacity is further developed.

5. Conclusions

This paper has described the test results of steel-concrete connection section structure of receiver tower. Through the analysis of the test results, the following conclusions are obtained.

（1）The connection section structure has experienced elastic stage, elastic-plastic stage and failure stage under low cyclic reciprocating load. Finally, due to the overall flexural yield of the upper steel frame and the local yield of the steel-concrete connection joints and longitudinal bars along the loading direction, the specimens were damaged.

（2）The hysteretic curve of the connection section structure generally presents an inverse S-shape after the structure yields. The hem and heu of the specimen under peak load and failure load are 0.215 and 0.261 respectively, indicating that the specimen still has a certain energy dissipation capacity after reaching the maximum bearing capacity.

（3）When the specimen is damaged, the stiffness of the specimen decreases to 1.3kn/mm and the strength degradation rate is 0.62, indicating that the stiffness and strength degradation of the specimen are serious.

（4）The displacement ductility coefficient of the specimen is as high as 9.2, which indicates that the connecting section structure has good ductility under the action of earthquake. The special structural form of connecting nodes can ensure the reliable connection between the upper steel frame and the lower concrete, and the whole structure will not be suddenly damaged, meeting the safety requirements.

Acknowledgments

This work was financially supported by National Natural Science Foundation of China (52078410) fund.

References

[1] J. Khan, M. H. Arsalan, Solar power technologies for sustainable electricity generation – A review, Renewable & Sustainable Energy Reviews, 2016, 55: 414-425.

ISSN:2790-1688 DOI: 10.56028/aetr.2.1.31
[2] S. S. Li, The characteristics of solar energy, Solar Energy, 2003(05): 10-12.

[3] D. A. Baharoon, H. A. Rahman, Z. Wan, et al, Historical development of concentrating solar power technologies to generate clean electricity efficiently – A review, Renewable and Sustainable Energy Reviews, 2015, 41(jan.): 996-1027.

[4] F. Guo, Y. K. Deng, Y. Q. Wu, et al, Shaking table test study on seismic performance of hybrid structure receiver tower, Industrial Construction, 2021, 51(03): 58-64.

[5] Q. Liu, Experimental study on seismic performance of high-rise solar receiver towers, Xi'an University of Architecture and Technology, 2018.

[6] S. J. Peng, Experimental study on seismic performance of solar thermal power tower under vertical earthquake, Xi'an University of Architecture and Technology, 2019.

[7] R. Zheng, Research on the dynamic characteristics of high-rise solar power tower, Xi'an University of Architecture and Technology, 2018.

[8] G. L. Bai, B. Hao, Strong earthquake response analysis of solar power tower with steel-reinforced concrete composite structure, Acta Energia Sinica, 2019, 40(06): 1503-1510.

[9] G. L. Bai, B. Hao, Research on seismic performance of steel-reinforced concrete tower composite structure under vertical earthquake, China Civil Engineering Journal, 2019, 52(03): 12-19.

[10] G. L. Bai, B. Hao, Shaking table test study of steel-reinforced concrete tower composite structure model, Journal of Building Structures, 2019, 40(12): 32-40.

[11] JGJ/T 101-2015, Specification for seismic test methods of buildings, Beijing: China Building Industry Press, 2015.

[12] G. L. Bai, F. H. Qin, Principle and design of steel reinforced concrete, Shanghai: Shanghai Science and Technology Press, 2002: 152.